

## Article

# Effects of Flaxseed Mucilage Admixture on Ordinary Portland Cement Fresh and Hardened States

Haris Brevet <sup>1,2</sup>, Rose-Marie Dheilly <sup>1</sup>, Nicolas Montrelay <sup>1</sup>, Koffi Justin Houessou <sup>1</sup>, Emmanuel Petit <sup>2</sup>   
and Adeline Goullieux <sup>1,\*</sup> 

<sup>1</sup> EPROAD-UR 4669, Université de Picardie Jules Verne, 80000 Amiens, France; harisbrevet@reseau.ispa.asso.fr (H.B.); rose-marie.dheilly@u-picardie.fr (R.-M.D.); nicolas.montrelay@u-picardie.fr (N.M.); houesfr@yahoo.fr (K.J.H.)

<sup>2</sup> BIOPI-UMRT BioEcoAgro, Université de Picardie Jules Verne, 80000 Amiens, France; emmanuel.petit@u-picardie.fr

\* Correspondence: adeline.goullieux@u-picardie.fr

**Abstract:** France is Europe's leading producer of flaxseed. This seed is rich in omega-3, energy, and protein for animals, but it also contains anti-nutritional factors such as mucilage. Thus, mucilage must be removed and could be used as a bio-admixture in cementitious materials development, reducing the environmental impact of cementitious materials. This study aims to valorize the usage of flaxseed mucilage (FM) in ordinary Portland cement. FM caused macroscopic and microscopic changes in the materials studied. The higher the concentration, the greater the changes were. The admixed samples showed an exponentially concentration-dependent delay in setting. FM degradation products induced by the cementitious conditions accentuated the delay. However, this delay in setting did not affect the hydrates' growth in the material. In fact, FM showed a "delay accelerator" behavior, meaning that once hydration began, it was accelerated as compared to a reference. Macroscopically, FM induced significant flocculation, increasing material porosity and carbonation. Consequently, bulk density and thermal conductivity were reduced. At the highest amount of FM admixture (0.75% *w/w*), FM allowed bridge formation between Ca(OH)<sub>2</sub> crystals, which can improve the mechanical properties of mortars. Because FM is highly hygroscopic, it has the capability to absorb water and subsequently release it gradually and under controlled conditions into the cement matrix. Therefore, regulation of water diffusion from the mucilage may induce the self-healing properties responsible for mechanical properties similar to that of the reference in the medium to long term.

**Keywords:** flaxseed mucilage; OPC; hydration; mechanical strength; FTIR; calorimetric analysis; SEM; alkaline degradation



**Citation:** Brevet, H.; Dheilly, R.-M.; Montrelay, N.; Houessou, K.J.; Petit, E.; Goullieux, A. Effects of Flaxseed Mucilage Admixture on Ordinary Portland Cement Fresh and Hardened States. *Appl. Sci.* **2024**, *14*, 3862. <https://doi.org/10.3390/app14093862>

Academic Editors: Mouhamadou Amar and Nor Edine Abriak

Received: 20 March 2024

Revised: 19 April 2024

Accepted: 25 April 2024

Published: 30 April 2024



**Copyright:** © 2024 by the authors. Licensee MDPI, Basel, Switzerland. This article is an open access article distributed under the terms and conditions of the Creative Commons Attribution (CC BY) license (<https://creativecommons.org/licenses/by/4.0/>).

## 1. Introduction

A sustainable agricultural and food approach aims at improving the nutritional quality of human food by balancing animal feed with forages and seeds naturally rich in omega-3s. Flaxseed is high in omega-3, energy, and protein, but it also contains anti-nutritional factors such as mucilage, which reduces nutrient digestibility and impacts broiler chicken growth [1]. France is Europe's leading producer of flaxseed, so its animal feed manufacturers want to improve the nutritional quality of the flaxseed by removing mucilage [2]. Therefore, it is necessary to find ways of adding value to mucilage, which is a by-product of the seed-dehulling process. One possibility would be to use it as a bio-admixture in cementitious materials.

Flaxseed mucilage (FM) is present in anhydrous form in flaxseed before hydration by contact with water. FM is a compound rich in polysaccharides (50–80%) but also in proteins (4–20%) and minerals (3–9%). FM is composed of two fractions of water-soluble heteropolysaccharides: the acidic rhamnogalacturonans type I (RG-I) fraction (17%) and

the neutral arabinoxylans (AX) fraction (83%) [3]. The bone composition of the mucilage varies according to the extraction conditions [4].

Rhamnogalacturonans are pectic acidic polysaccharides that can impact cement hydration and cementitious properties. Shanmugavel et al. [5] observed a consistency decrease and longer setting times with the increase in pectin percentage. They stated that during the hydration of cement paste, the galacturonic acid can form strong intermolecular association among the galacturonan chains by forming calcium bridges, with the effect of enhanced viscosity. According to Thomas and Birchall [6], natural polymers have the inherent characteristic of surface absorbency of organic molecules and subsequent development of protective polymeric film on the cement particles and hydration products. This film would restrict further hydration of cement particles. Hazarika et al. [7] also observed the viscosity-enhancing property of the addition of acidic heteropolysaccharides but a setting time reduction. As pectin incorporates some amount of calcium ions in its structure during the hydration of cement, the  $\text{Ca}^{2+}$  concentration in pore fluid would decrease. To balance the  $\text{Ca}^{2+}$  concentration, the rates of the hydration of cement minerals would increase, and greater amounts of hydration products would be formed, resulting in a decrease in setting times. Pan et al. [8] used carrot extract, whose main polysaccharide is rhamnogalacturonan. They observed a delay in setting and an enhanced compressive strength of the mortars. The positive effect on the compressive strength would be due to greater development of Portlandite and C-S-H in the cementitious system.

Concerning the arabinoxylans, a neutral fraction of polysaccharides, Girones et al. [9] observed a retardation of cement hydration with 2% (*w/w*) of AX. The AX polymers might slow down not only the formation but also the growth of the C-S-H nuclei. The impact of rhamnogalacturonans and arabinoxylans on cement seem to be dependent on the polysaccharide concentration and other compounds present in the extracts.

One of the plants used in its extract form as a replacement for mixing water is *Opuntia ficus indica* (OFI)—its availability, low operating cost, and presence in arid areas where water is most needed make it an important element in cement admixture. OFI cladodes are waterlogged and contain a huge amount of polysaccharides and some proteins that probably can interact with the complex hydration mechanism of Portland cements [10,11]. But this extract used for water mixing in cement contains a percentage of mucilage and proteins but also some other natural compounds (cellulose, fats, hemicellulose, starch, ashes, etc.) [5,12]. Chandra et al. [11] indicated that the incorporation of OFI extract increases the plasticity of the cement paste with a consequent decrease in water absorption by the mortar and an improvement in the freeze–thaw resistance of the mortar. The author also showed a possible interaction between the polysaccharides and the Portlandite formed. The formation of complexes influences the crystallization process, interfering with the size of the Portlandite crystals and making them more amorphous. The ability of OFI polysaccharides to interfere with the growth of mineral species and the crystal microstructure was confirmed using several polysaccharides [13]. Finally, the addition of polysaccharides within a cementitious matrix reduces the carbonation phenomenon of the material by acting as a barrier property to gases and water, a property conferred by the viscous extract of OFI [10,11]. Not all polysaccharides have the same resistance to the highly alkaline cementitious environment. Polysaccharides added to the cementitious matrix degrade more or less easily into hydroxycarboxylic acids or smaller entities.

The objective of the present study was to investigate the impact of the admixture of FM at different concentrations in a cement matrix. An evaluation of the FM degradation in an alkaline environment is herein discussed. A fresh state study of Portland cement provided some understanding of the hydration properties of cement in the presence of FM polysaccharides. The mechanism and products of hydration were investigated in the fresh state and in the hardened state after different curing times. The impact of the admixture rate on the macroscopic and microscopic structure was also explored in this study to obtain a more comprehensive knowledge of the impact of the addition of mucilage on the growth

of hydration products. To this end, mortars were manufactured, and their mechanical strengths and thermal conductivities were evaluated.

## 2. Materials and Methods

### 2.1. Materials

The cement used in this study was an Ordinary Portland Cement (OPC), CEM I 52.5 N CE PM-CP2 NF, commercialized by Calcia, Courbevoire, France. The clinker is the main component ( $\geq 95\%$  *w/w*) of this cement, and no fillers were applied in this study, so result dispersion was avoided. Its composition in weight % is 74.8, 3.7, 8.2, and 8.3 for  $C_3S$ ,  $C_2S$ ,  $C_3A$ , and  $C_4AF$ , respectively. The Bogue approximation gives 66.48, 20.97, 4.84, 2.73, 3.4, and 0.21% (*w/w*) for CaO,  $SiO_2$ ,  $Al_2O_3$ ,  $Fe_2O_3$ ,  $SO_3$ , and  $Na_2O$ , respectively. It exhibits a Blaine fineness of  $4360\text{ cm}^2\cdot\text{g}^{-1}$ . The different mortars were elaborated with a 0/4 mm sand, according to the NF EN 12620 standard. With respect to the French standard NF EN 1008, the mixing water used in this study was tap water at a temperature of  $20\text{ }^\circ\text{C} \pm 2\text{ }^\circ\text{C}$ . Flaxseed mucilage (FM) used as admixture originated from a gold flaxseed cultivar (Eurodor) and is available in a lyophilized form after the extraction procedure described by Brevet et al. [14].

### 2.2. Flaxseed Mucilage Characterization

#### 2.2.1. Determination of FM Proximate Composition

The protein content of FM was quantified according to the Kjeldahl method described by AOAC 954.01 [15] on the determination of total nitrogen content in the samples. A conversion factor of 6.25 was used to calculate the crude protein content from the nitrogen content.

The AOAC Official Method 942.05 was used to determine the ash content of FM. An approximate 2 g of raw materials was weighed in porcelain crucibles and then calcined at  $600\text{ }^\circ\text{C}$  for 2 h in a pre-heated muffle furnace. The cooling step of the calcined samples was different from the AOAC method. The calcined materials were cooled in an oven at  $70\text{ }^\circ\text{C}$  for 2 h to avoid any moisture regain before being weighed.

High-performance anion-exchange chromatography with pulsed amperometric detection (HPAEC-PAD) was used to determine the FM monosaccharides composition and content. Results are expressed in grams of carbohydrates/100 g of FM. The analysis was performed as described by Roulard et al. [16].

#### 2.2.2. Alkaline Solubilization of FM

The solubilization of FM in alkaline solutions allows the evaluation of the impact of the pH and the presence of  $Ca^{2+}$  cations on the availability of the characteristic groups of polysaccharide chain length after solubilization. The mucilage was dissolved (2, 5, 10, 15, 20, 25, and 30 g/L) into two different solutions of pH = 12.6: NaOH 0.04 M and  $Ca(OH)_2$  0.02 M. Solubilization was carried out at a rotation speed of 140 rpm in a beaker with a paddle stirrer until complete mucilage solubilization occurred to simulate the slow speed of mixing in an alkaline environment of the standard EN 196-1 [17] relative to mortar development. Then, alkaline mucilage solutions were dried in an oven at  $50\text{ }^\circ\text{C}$  to avoid any degradation due to temperature. Fourier transform infrared spectroscopy (FTIR) and viscosity measurements were carried out to evaluate the alkaline environment impact on FM.

#### 2.2.3. Apparent Viscosity of FM

The viscosity range of mucilaginous solutions was established using a rheometer (DVNext, Brookfield, Toronto, ON, Canada) with appropriate HA/HB spindles ranges. Mucilaginous solutions were prepared to obtain seven solutions at different concentrations (2, 5, 10, 15, 20, 25, and 30 g/L) by solubilizing FM into tap water, NaOH 0.04 M, and  $Ca(OH)_2$  0.02 M at 400 rpm until all the FM was solubilized. The viscosity values were obtained at different spindle rotational speeds from 20 to 200 rpm. The designated viscosity

value corresponds to a constant rotational speed of 60 rpm, corresponding to the most adequate torque generated for all solutions. At 60 rpm, the torque value during the experiment was optimal (between 40 to 60% of the maximum torque tolerated by the instrument). At higher speeds, the torque was in the low range of the apparatus, while torque values that were too high were obtained at speeds lower than 60 rpm.

#### 2.2.4. FT-IR Characterization

Fourier transform infrared spectroscopy was used to characterize the changes in FM following alkaline solubilization. Dried FM materials were analyzed. The FTIR spectra of FM were determined by FTIR spectrophotometer (IR-Prestige 21, Shimadzu, Noisiel, France). Approximately 1% (*w/w*) of FM was weighed and crushed on a KBr matrix pellet (200 mg). The FTIR spectra were obtained with 200 scans in a transmittance mode and a resolution of 2.0, where an Happ–Genzel apodization was applied in a range of 400–4000  $\text{cm}^{-1}$ .

#### 2.3. Mortars Preparation

The preparations are carried out in a standardized mortar mixer (EN 196-1) (Proviteq, Lisses, France). FM was incorporated by solubilizing within the mixing water to fully study the interaction between the polysaccharides and the cement. Mortars were elaborated with a W/C ratio of 0.5 according to EN 196-1. The mortar compositions are given in Table 1. The samples were molded without the use of an impact table. The objective was to study the macroscopic structural effect of mucilage on a cementitious mortar. The molds used have dimensions of  $4 \times 4 \times 16$  cm for the study of the mechanical strength and  $10 \times 10 \times 2$   $\text{cm}^3$  for the further thermal conductivity study of mucilage-admixed materials. Each sample for strength tests was then cured for 28, 60, and 90 days (Table 1) in a chamber with saturated humidity and at room temperature. The samples for the thermal conductivity measurements were cured for only 28 days. Before characterization, samples were dried in an oven at 50 °C until a constant mass was obtained.

**Table 1.** Polysaccharidic mortars compositions.

Sample	Water (g)	Solubilized Mucilage (g)	Admixture (% Cement)	Cement (g)	Sand (g)	Curing Time (Days)
OPC	225	0	0	450	1350	28, 60, 90
EURO2G	225	0.45	0.1	450	1350	28, 60, 90
EURO5G	225	1.125	0.25	450	1350	28, 60, 90
EURO15G	225	3.375	0.75	450	1350	28, 60, 90

#### 2.4. Characterization of FM Admixed Mortars

##### 2.4.1. Setting Times Determination

The evaluation of the hydration heat release is an effective technique for monitoring the hydration process and determining the initial and final setting times of pastes containing different amounts of FM. The experiments were conducted on a Calvet calorimeter C80, Setaram. Pastes were prepared by mixing 100 g of cement with 50 g of the mixing tap water at different mucilage solution concentrations (0, 2, 5, 15, and 30 g/L). The cement and water mixture were homogenized with an electric whisk during a 30 s time minimum depending on how difficult it was to homogenize the mix. Then, an approximate 3000 mg of each paste was introduced into a stainless-steel capsule. The heat flow ran for a minimum time of 48 h in a  $25 \pm 0.5$  °C regulated chamber.

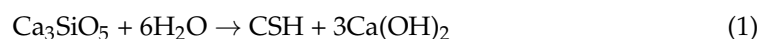
##### 2.4.2. Slump Test

The slump test was performed on a mini-Abrahams cone called MBE (“Mortier Béton Equivalent” translated as “Concrete Equivalent Mortar”), which has dimensions of 150 mm height and an upper and lower diameter of 50 and 100 mm, respectively. The test was carried out following the procedure described by Schwartzenruber et al. [18].

### 2.4.3. Hydration Degree

When the major cement compounds, i.e., tricalcium silicates ( $C_3S$  Equation (1)) and dicalcium silicates ( $C_2S$  Equation (2)), are in contact with water, there is formation in the first few hours of calcium silicate hydrate (also called C-S-H), ettringite, and Portlandite ( $Ca(OH)_2$ ). Over time, it is possible to form calcium carbonate ( $CaCO_3$  Equation (3)) in various forms—calcite, vaterite, and aragonite. These different compounds are dependent on the hydration of the cement grains. To quantify good cement hydration, Bhatti developed a method based on thermogravimetric analysis [19]. The thermogravimetry allows the degradation of the hydration products by dissociation reactions—dehydration for C-S-H (Equation (4)), dehydroxylation for Portlandite (Equation (5)), and finally, decarbonation for calcium carbonates (Equation (6)).

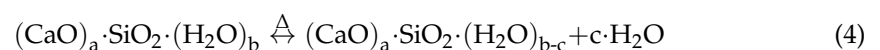
The hydration reaction of tricalcium silicates and dicalcium silicates is as follows:



That for Portlandite carbonation with ambient carbon dioxide is as follows:



The first reaction of CSH dehydration is given below [20]:



The second reaction of dehydration or dehydroxylation of Portlandite is as follows:



The decarbonation reaction of the calcium carbonate phases occurring at higher temperature is given below:



The method developed by Bhatti [19] allows determining the degree of hydration (DH) of mortars and cement pastes, taking into account the different dissociation reactions. The Equation (7) is used to determine the DH, according to the author.

$$DH(\%) = \frac{W_b}{0.24} \times 100 \quad (7)$$

where  $W_b$  corresponds to the chemically bound water, and 0.24 corresponds to the part of chemically bound water that is combined with each part of cement.  $W_b$  (Equation (8)) quantifies the weight loss during the dehydration (Ldh), the dehydroxylation (Ldx), and the decarbonation (Ldc). The correction coefficient 0.41 is based on the assumption that carbonate is formed only by the reaction of  $CO_2$  with  $Ca(OH)_2$  [21].

$$W_b = (Ldh + Ldx) + 0.41(Ldc) \quad (8)$$

A differential scanning calorimetry coupled with thermogravimetric analysis (DSC-TGA) (Themys LV, Setaram, Caluire-et-Cuire, France) was carried out on cement mortars and pastes to determine their degree of hydration and thus to evaluate the FM action on the evolution of the hydration products. The mortars were powdered using a mixer mill (MM400, Retsch, Eragny, France). About 130 mg of this powder was introduced into porcelain crucibles. The analysis started at 25 °C and went up to 1100 °C at a rate of 5 °C/min under a helium atmosphere.

#### 2.4.4. Mechanical Characterization of Mortars

The strengths of the mortars were determined in compression at different curing times (28, 60, and 90 days) on a machine from Proviteq, France, with a load cell threshold of 100 kN. The strengths were obtained at a load rate of  $2400 \text{ N}\cdot\text{s}^{-1}$  on twelve replicates according to the EN 196-1 standard.

#### 2.4.5. Microstructure Visualization

The morphology of the samples was studied using scanning electron microscopy (namely SEM). This analysis allowed visualizing the macro and microporosities of the different mortars. The micrographs were obtained using a PHILIPS FEG XL 30 microscope. To facilitate observation, the samples were first dried and then coated with a thin layer of spray-on gold to enhance their electric conductivities. SEM observations were coupled with an energy dispersive X-ray spectroscopy (EDS) analysis allowing the surface samples' elements identification.

#### 2.4.6. Thermal Conductivities Determination of Mortars

The samples ( $10 \times 10 \times 2 \text{ cm}^3$ ) were cured for 28 days and then analyzed by transient plane source (TPS) 2500, HotDisk, to determine their thermal conductivities. Before measurements, the samples were dried in an oven at  $50 \text{ }^\circ\text{C}$  for at least a week until a constant mass was obtained. Measurements were repeated three times.

### 3. Results and Discussion

#### 3.1. FM Characterization

##### 3.1.1. Proximate Composition of FMs

The proportion of protein is 10.3%, and the quantity of carbohydrates is 45.1% mass of mucilage. The extracted product is relatively clean since the ash content (3.8%) is relatively low compared with values found in the literature [3,4,16,22,23]. All these values are highly affected by the process parameters [4,24] and the flaxseed cultivar [3].

The polysaccharide composition is categorized into two distinct fractions. The neutral fraction consists of xylose and arabinose, forming arabinoxylans (AX). This fraction accounts for 72% of the total polysaccharides. The second fraction, constituting 28% of the polysaccharide content, is an acidic fraction primarily composed of rhamnose and galacturonic acid, resulting in type I rhamnogalacturonans (RG-I). Warrand [25] initially elucidated this mucilage separation into these two fractions. He noted that the neutral and acidic fractions make up approximately 75 and 25% of the polysaccharide content in mucilage, respectively.

Finally, it is interesting to look at one of the mucilages that was referenced as a bio-admixture and whose admixture effects on the characteristics of cementitious matrices are widely praised and positive. The Table 2 shows an interesting parallel between the monosaccharide composition of the FM and OFI cladode mucilage. It is clearly visible that the monosaccharide profiles are completely different, with a large presence of galacturonic and glucuronic acid for OFI. The large presence of a pectic fraction greatly differentiates it from FM, where 73% of the content is a neutral fraction. It is therefore possible that FM does not have the same effects on cement materials as OFI mucilage.

**Table 2.** Monosaccharides content (g sugar/100 g) of FM and OFI cladodes.

Monosaccharide	HPAEC-PAD FM (Raw) <sup>1</sup>	FM <sup>3</sup>	OFI <sup>4</sup>
Galacturonic acid	$3.686 \pm 0.708$	8.17	23.2
Arabinose	$8.580 \pm 0.373$	19.02	18.8
Galactose	$5.857 \pm 0.165$	12.98	31.8
Glucose	$1.910 \pm 0.106$	4.23	25.1
Fucose	$1.673 \pm 0.038$	3.71	
Rhamnose	$7.751 \pm 0.169$	17.18	

Table 2. Cont.

Monosaccharide	HPAEC-PAD FM (Raw) <sup>1</sup>	FM <sup>3</sup>	OFI <sup>4</sup>
Xylose	15.640 ± 0.984	34.67	1.1
Glucuronic acid	0.009 ± 0.003	0.020	23.2
TOTAL	45.105 ± 1.793 <sup>2</sup>	100	100

<sup>1</sup> Raw data obtained from the HPAEC-PAD. <sup>2</sup> The sum of compounds does not reach 100% due to carbohydrates losses during the HPAEC-PAD hydrolysis [26]. <sup>3</sup> First column monosaccharides content on 100% basis to compare with OFI. <sup>4</sup> Values from Lefsih et al. [27].

### 3.1.2. Impact of Alkaline Conditions on FM

**Apparent viscosity:** When the mucilage is dissolved in the mixing water, the pectic and neutral fractions interact and structure themselves to form a more or less viscous network, depending on the concentration. This viscosity was therefore determined at different mucilage concentrations and is used as a reference for determining the quantity added to the cementitious matrix. It is also possible to simulate the effect of the cementitious matrix on the composition and/or degradation of polysaccharides using viscometry. The viscosimetric behavior of polysaccharides dissolved in different alkaline solutions (NaOH and Ca(OH)<sub>2</sub>) with a deliberately high pH, such as the cementitious medium, can be seen in Figure 1.

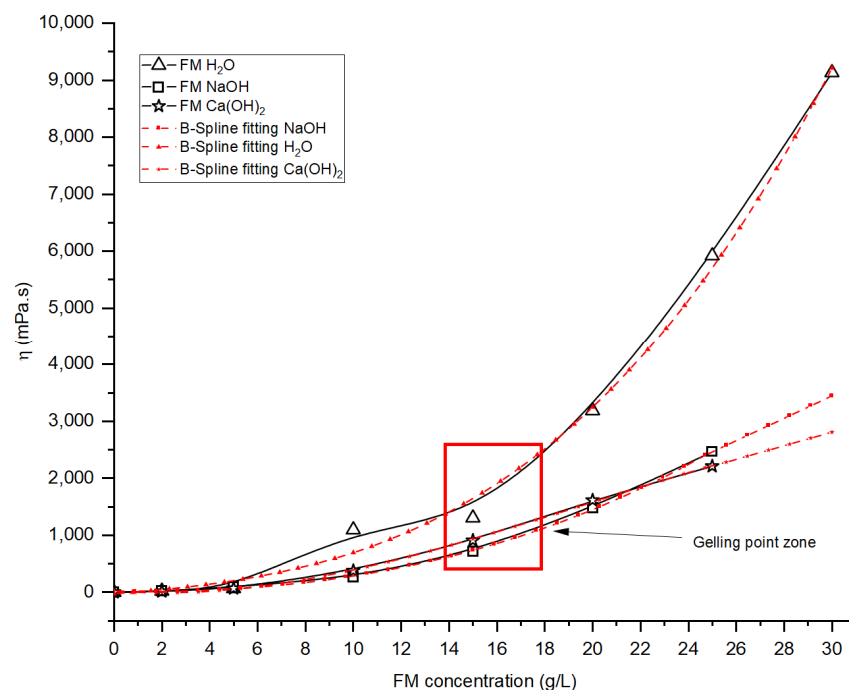


Figure 1. Apparent viscosity of FM solutions at  $20 \pm 2$  °C (60 rpm).

Firstly, Figure 1 shows that the viscosity of the FM increases significantly as a function of the FM concentration. This increase is accelerated at around 15 g/L. This concentration was identified as a gelling point or a sol–gel transition [25]. Warrand [25] conducted a study on the viscous properties of FM and found that FM exhibits shear-thinning behavior. This means that the viscosity increases with increasing polysaccharide concentration, primarily due to interactions between the two distinct fractions present in FM. The pectic fraction that is anionic has minimal or no impact on determining the solution's physicochemical properties. Instead, it is mainly the neutral fraction, primarily composed of AX, that is responsible for the exceptionally high viscosity of the mucilage solution. The gel-forming characteristics of the AX solution arise from intermolecular hydrogen bonds and a relatively larger molecular weight compared to the acidic fraction. Several studies have reported

a critical transition point in the apparent viscosity of the mucilage solution [4,25]. Like many plant extracts [28,29], this sol–gel transition point corresponds to the concentration or condition at which the solution ceases to be considered a true solution and instead behaves as a gel. This transition occurs due to the increasing entanglement of polymeric chain networks, which restricts the mobility of the polysaccharide chains and leads to a significant increase in viscosity [25].

FM does not exhibit the same behavior when added in alkaline conditions, as shown by the Figure 1. The viscosity curves part ways with the aqueous medium from a 5 g/L concentration. The apparent viscosity increases with the concentration but much less for the alkaline solutions than in water. There are two possible explanations for these observations.

First, the intermolecular network formed by hydrogen bond is reduced due to the action of NaOH and Ca(OH)<sub>2</sub> solutions. Chen et al. [30] worked on the gelation properties of flaxseed gum and confirmed the results shown in Figure 1. Flaxseed gum is characterized by its anionic polysaccharide nature, resulting from the presence of ionized carboxyl groups that generate a negative charge. The electrostatic forces between like-charged molecules cause the molecular chains to fully extend and intertwine, facilitating the formation of intermolecular cross-links that induce gelation at pH between 6 and 9. The authors explained that increasing the pH above 9 diminishes the gel strength and thus the apparent viscosity. Furthermore, they also mentioned that the Na<sup>+</sup> action on the zeta potential leads to a decrease in the intramolecular charge repulsions. The same mechanism of electrostatic repulsion exists with a large amount of divalent cations like Ca<sup>2+</sup>, which inhibits the formation of a three-dimensional network [30]. The presence of divalent cations in a lower concentration can, however, induce a cross-linking or flocculation of the polysaccharides, as we observe a sedimentation because of agglomerates' formation. These phenomena are visible in Figure 1, as the NaOH and Ca(OH)<sub>2</sub> solution curves flatten compared to that for water. A higher flattening on the Ca(OH)<sub>2</sub> curve can be evidence of a divalent cation intermolecular cross-linking, shown by a flocculation visible during the material preparation.

The second hypothesis that can lead to the apparent lowering of viscosity concerns the possibility of polysaccharide degradation. In our conditions, molecular weight determination by SEC-MALS analysis does not demonstrate backbone hydrolysis (Figures S1 and S2). This hypothesis is not consistent with our results.

Thus, in NaOH and Ca(OH)<sub>2</sub> solutions, the decline in gel strength is linked to fewer junction zones due to high pH levels (pH > 9) and the presence of monovalent and divalent cations, as reported by several authors [31–33].

Compositional modifications—FTIR: The FM solubilized under different conditions were analyzed in FTIR to determine possible compositional modifications. The FTIR spectra are visible in Figure 2. First, there is an appearance of a doublet at 897 and 866 cm<sup>-1</sup> when alkaline conditions are applied to the FM. These bands are characteristic of the co-existence of β- and α-glycosidic bonds [34], respectively. This new co-existence is possible evidence of an alkaline hydrolysis, as alkaline catalysts are often used to liberate carbohydrate chains from glycoconjugates [35]. The liberation of glycoconjugates such as proteins is visible on the NaOH solution spectrum with the disappearance of the N-H bond at 1541 cm<sup>-1</sup>. Also, the C-H “hairy zone” and -CH<sub>2</sub> branched at 1413 cm<sup>-1</sup> look different. The increase in the band and the apparition of a triplet at 1444, 1413, and 1382 cm<sup>-1</sup> seem to confirm the hydrolysis of the side-branched conjugates. In the Ca(OH)<sub>2</sub> FM solution, this N-H bond seems to still be present, as the divalent cation can bind different polysaccharidic/protein compounds and then limit the impact of alkaline solution as characteristic groups are protected.

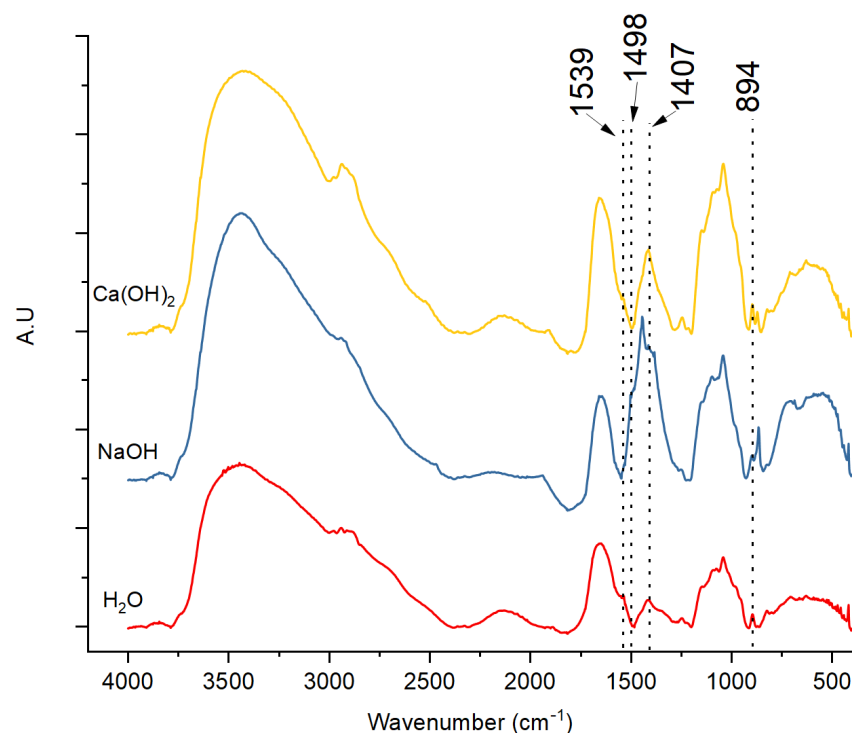


**Figure 2.** Infrared spectra of solubilized mucilages at different alkaline conditions.

The complexification and increase in organic species present in the cementitious medium after the FM degradation make it more complicated to conduct studies and to identify the mechanisms intrinsic to the initial polysaccharides. For example, Kang et al. [36] related that xylose, which is the main saccharide of the FM, degrades mainly to formic acid and furfural. Whistler and BeMiller [37] described the alkaline degradation process of polysaccharides as a peeling process in which the reducing end-group is liberated from a chain by elimination of the rest of the chain as a glycoxy anion.

### 3.2. Characterization of Cement Composites

#### 3.2.1. Fresh State Characterization

**Slump test:** The elaboration of mortars requires characterization in the fresh state to determine the workability and viscosity of the hydraulic material. This measurement is all the more relevant when an admixture is incorporated. Figure 3a,b show the consistency of a EURO5G admixed mortar and the values obtained from the slump test, respectively. Figure 3a clearly shows the appearance given by the mucilage to the material. The addition of FM to a cementitious composite tends to form flocks whose size and shape depend on the mucilage concentration. The size decreases as the concentration increases, and the sphericity of these aggregates becomes more regular as the mucilage concentration increases. This particular granular structure suggests a coating of the cement grains/sand by the polysaccharide and not an increase in workability, as may be the case with OFI mucilage [11,38]. This important granular aspect makes the cement particularly dry (in conditions of  $W/C = 0.5$ ) and difficult to work. During samples molding and demolding, this granular aspect, bordering on sandy, makes the material quite friable. As mucilage is a very hygroscopic material, the water available for hydration during mixing may be reduced initially. Dissolving the mucilage also allows the polysaccharide chains to unwind and ionize. This ionization makes the anionic groups available to bind with the metallic cations present in the cement, as shown previously with the FM solubilization in alkaline solutions and FTIR conclusions. This interaction at the surface of the cement grains has been shown to be an absorption or adsorption of the polysaccharide groups onto the cement grains, resulting in a flocculation process [39]. This phenomenon can be seen in Figure 4. Moreover,

the kinetics of cement hydration makes this phenomenon even more plausible. Indeed, due to the substantial water absorption by the mucilage and the cement's affinity for water, the hydration kinetics of the cement enable the formation of this bond. Figure 4 shows that the greater the amount of mucilage, the greater the flocculation.

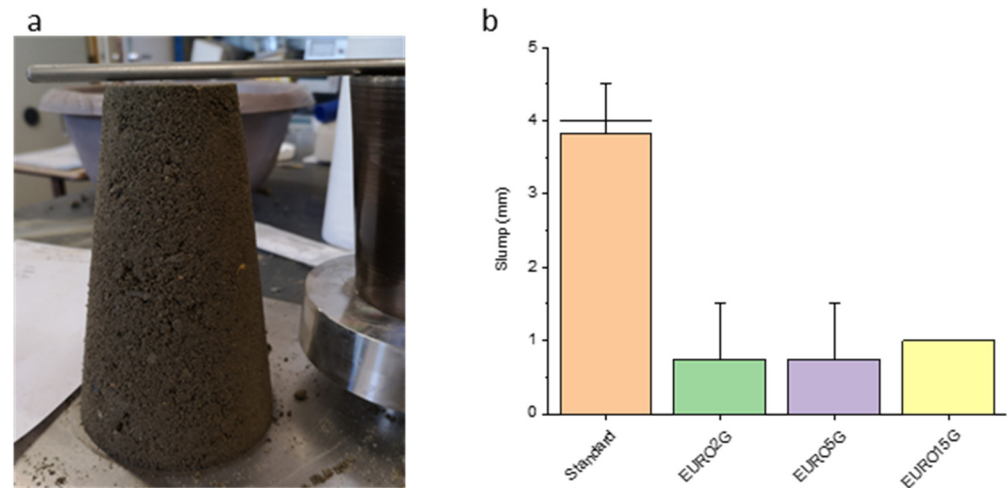


**Figure 3.** Slump test (a) of the mortars and the results (b).

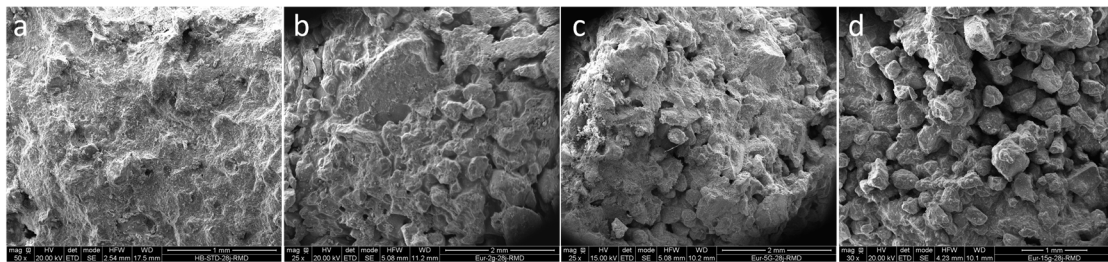


**Figure 4.** Granular shape of 28 days cured mortars—(a) reference, (b) EURO2G, (c) EURO5G, and (d) EURO15G.

**Setting times determination:** The polysaccharide has the ability to bind with cement cations and absorb an amount of mixing water necessary to the cement for hydration and hardening. The Figure 5 illustrates the isothermal calorimetry of the polysaccharide admixed cement pastes. Zhang et al. [40] worked on the retarding effect of saccharides on cement pastes and concluded that the initial and final setting times increased exponentially as a function of the sugar concentration. To confirm these results, an additional cement paste, with 30 g/L mucilage mixing water (1.5%  $w/w$  cement), was used. The results are shown in Figure 5a–c.

The Figure 5a clearly shows the impact of the polysaccharides on the cement hydration. The setting times, both initial and final, are increased as a function of rising polysaccharides concentration. The polysaccharides also influence the heat generated during the hydration and extend the induction period. The Figure 5c confirms the conclusions of Zhang et al. [40] that the setting is exponentially influenced by the polysaccharides concentration. Figure 5b shows a crossing point of the admixed cement pastes curves with the reference one around 32 h, indicating a higher hydration rate above that crossing point for the admixed cement pastes. Zhang et al. [40] mentioned this point. Moreover, after 48 h of hydration, excepted for EURO15G and EURO30G, the cumulated heat is at least similar or higher than that of the reference.

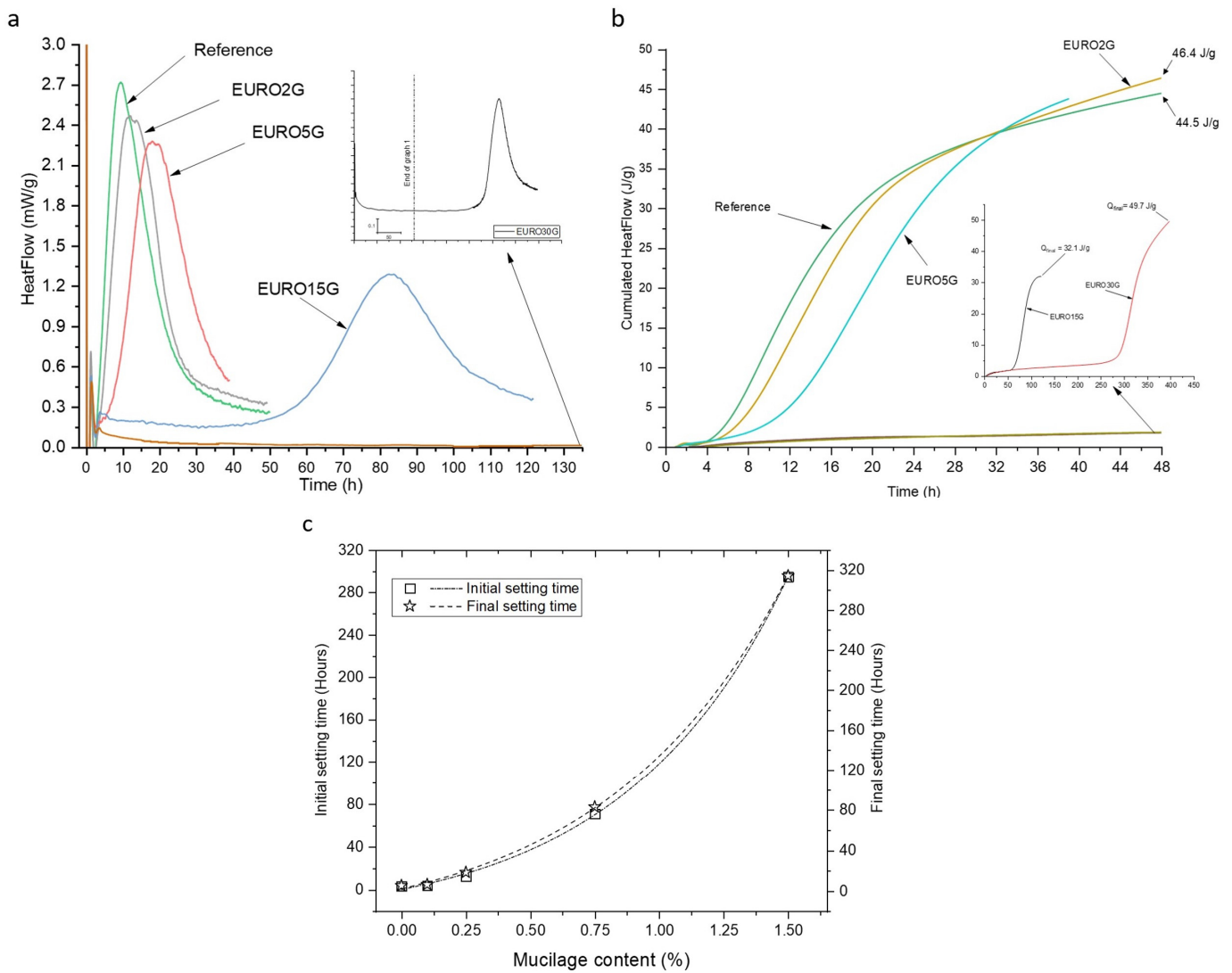


**Figure 5.** Setting times determination of mucilaginous cement pastes at  $W/C = 0.5$  ((a) heat flow versus time according to mucilage content, (b) cumulated heat flow versus time according to mucilage content, and (c) initial and final setting times versus mucilage content).

Another evidence of the polysaccharide impact is on the mineral activity. The first part of the hydration process is characterized by a linear curve (Figure 5b). Before the deceleration of the hydration process, the slopes of the integrated curves are 2.49, 2.37, 2.19, 0.84, and 0.68  $\text{h} \cdot \text{g} \cdot \text{J}^{-1}$  for the standard, EURO2G, EURO5G, EURO15G, and EURO30G, respectively (upper and lower bounds are:  $X = [7.3; 16.7]; [9; 18.9]; [12.9; 24.4]; [67.2; 98]; [296.3; 329.4]$  for the standard, EURO2G, EURO5G, EURO15G, and EURO30G, respectively). All the evidence of the crossing point, the higher ending heat generated, and the lower slope during the induction period highlight the acceleration of the hydration process at the end of the 48 h, which was confirmed by the work of Zhang et al. [40]. For these authors, this behavior (called “delayed acceleration”) is consistent with the fact that the induction period is controlled by slow formation or poisoning of the CSH nuclei [40] induced by the FM.

For EURO15G and EURO30G, the mineral activity is very low as the induction period is increased. FM is composed by AX, which is a neutral fraction, and by RG, which is the anionic one. In the neutral fraction, especially at the anomeric carbon (C1) of the end reducing units, the HO-C-C1=O groups of the arabinose and xylose [41] but also the  $\alpha$ -hydroxylated acid as galacturonic acid units in the RG fraction [42] have the ability of binding with the cement dissolved ions, thus limiting the CSH nucleation at the surface of the cement grain. The increasing setting times and induction period as the polysaccharide concentration rises is the result of a co-action of chemisorption of the metallic ions from the cement and the increasing viscosity of the paste at higher polysaccharide concentrations. This high viscosity, provoked by an increasing amount of unwound polysaccharides, generates more cement grains ions absorption and an important reduction in mobility of those ions caused by a steric hindrance. It has the effect of lowering the rate of the CSH nucleation and  $\text{Ca}(\text{OH})_2$  precipitation (Figure 6). This point is confirmed by combining viscosity measurements of FM solutions and setting time measurements of the admixed cement pastes.

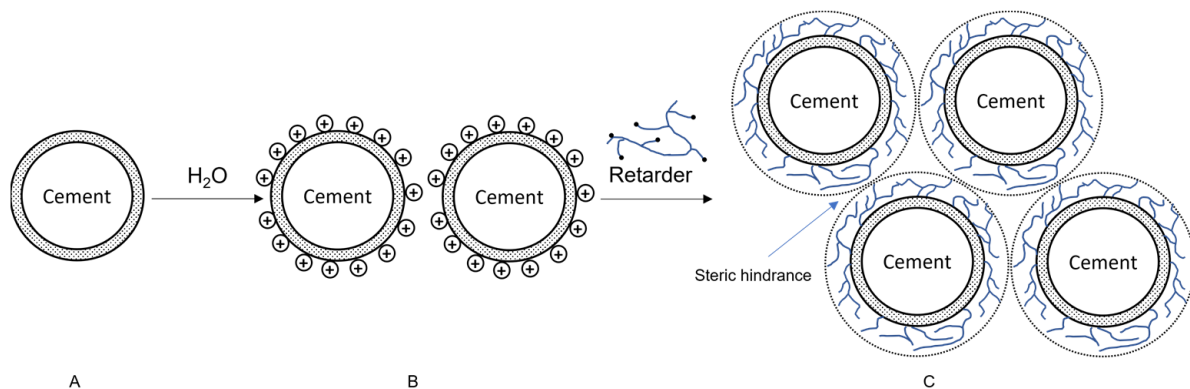


**Figure 6.** Schematic representation of the retardant barrier formation mechanism and the increase in steric hindrance. (A) Anhydrous cement grain, (B) formation of cationic sites on the surface of the cement grain, and (C) bonding of retarder and formation of a semi-permeable barrier around the cement grains.

### 3.2.2. Evaluation of the Hydrates Formed in Cement Mortars

Figure 7a shows the compressive strength and bulk density of mortars aged from 28 to 90 days, with their respective degrees of hydration shown in Figure 7b. It can be seen from this figure that the compressive strength evolves constantly over time and in the same way as the bulk density, which is not the case for the degree of hydration. The EURO2G and EURO5G mortars yield a strength that is identical or close to the reference, but the maximum strength seems to be reached after 60 days and then no longer evolves. Lastly, EURO15G shows weaknesses in compressive strength despite a significant change in strength over time compared to the other samples. For the same curing time, the higher the addition of FM, the lower the bulk density. The degree of hydration is at least identical to that of the reference but higher. This indicates good hydration of the hydraulic binder over time. These elements highlight the macroscopic granular, sandy shape of the mortar (Figure 4) caused by flocculation, which is responsible for the weakness of the material.

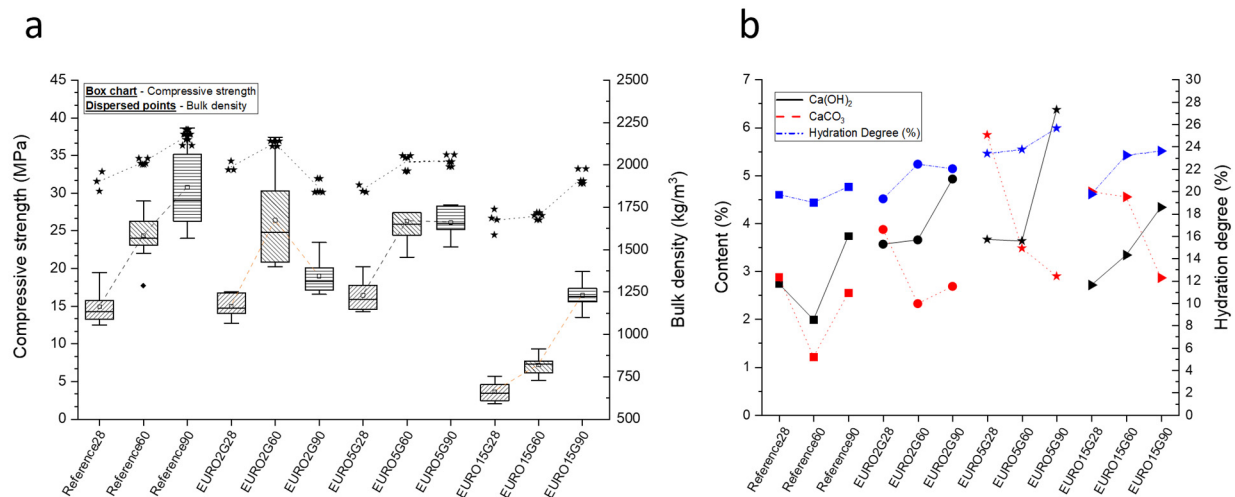


**Figure 7.** Compressive strength and bulk density (dispersed stars) (a) and hydration degree and hydrates contents (b) of 28-, 60-, and 90-day cured mortars.

For EURO2G and EURO5G, Figure 7b shows the quantity of hydrates developed at different curing times. The evolution of the quantity of Portlandite and CaCO<sub>3</sub> over time are the opposite, indicating a dissolution of the carbonates by prolonged hydration over time. This trend is not observed with the reference, in which the evolution of Portlandite and carbonates are linked. These results suggest that mucilage promotes carbonation at young ages and, further, the presence of Portlandite by prolonged hydration. This phenomenon has been described for certain polysaccharides in the case of self-healing concretes [43,44]. The increase in the carbonation of cement at young ages is favored by various factors, either jointly or independently:

- The degradation of mucilage into alcoholic saccharides, which promote the formation of calcium carbonate;
- The presence of -COO<sup>-</sup> carboxyl groups within the mucilage and the accumulation of Ca<sup>2+</sup> on the surface of the cement grains increase the conditions for the bond between CO<sub>3</sub><sup>2-</sup> and Ca<sup>2+</sup> ions. These conditions favor the precipitation and crystallization of CaCO<sub>3</sub> [45];
- The increase in mucilage concentration leads to an increase in grain flocculation and a decrease in the compactness of the cementitious matrix. The porosity created by the macro-structure of the composite can lead to a deeper access of ambient CO<sub>2</sub> into the material and thus to carbonation at an early age. This argument is validated by the work of Wang et al. [46];
- The viscosity confers a bubble trap characteristic to the mucilage. The higher the viscosity, the stronger this characteristic. During the mucilage solubilization and mixing phase, the air bubbles contained in the mucilage entrap a significant quantity of O<sub>2</sub> and CO<sub>2</sub> from the ambient air in particular. These gases find their way into the cementitious matrix at early ages, encouraging the formation of CaCO<sub>3</sub> [47,48].

When FM is added in the matrix, the high amount of calcium carbonates formed in the first ages is followed by a decrease. FM is able to capture water in the ambient air as a high hygroscopic material. The captured water will diffuse slowly and in a controlled manner over time into the cement matrix, which may lead to a long-term hydration. This long-term hydration induced by the FM corresponds to the rise in the amount of Portlandite in Figure 7b.

### 3.2.3. Microstructure Visualization—SEM

Figure 8 shows SEM images of the mortars at 28 days and 90 days. The matrices and the matrix/sand interfaces enable the evaluation of the evolution of the material over time

as well as the adhesion of the matrix to the sand grain. According to these images, the adhesion of the matrix to the sand grain evolves negatively from the reference to EURO15G, with interfacial transition zones of 0  $\mu\text{m}$ , 0.2–0.3  $\mu\text{m}$ , 0.3  $\mu\text{m}$ , and 0.5–1.4  $\mu\text{m}$  on average for the reference, EURO2G, EURO5G, and EURO15G, respectively. These values are the second argument that the compressive strength of mortars decreases as the mucilage concentration increases after the flocculation by polysaccharides, as shown in Figure 4.

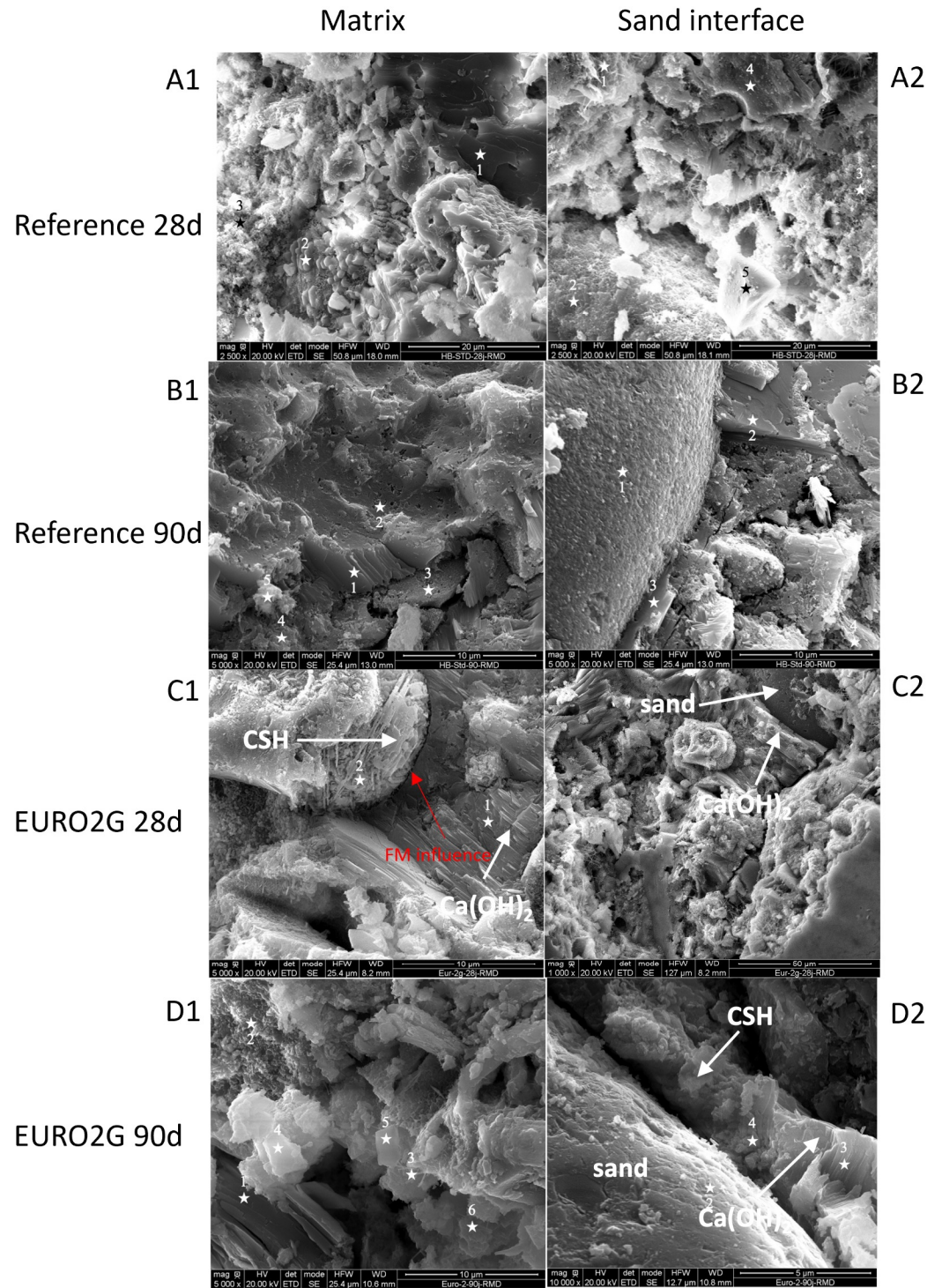
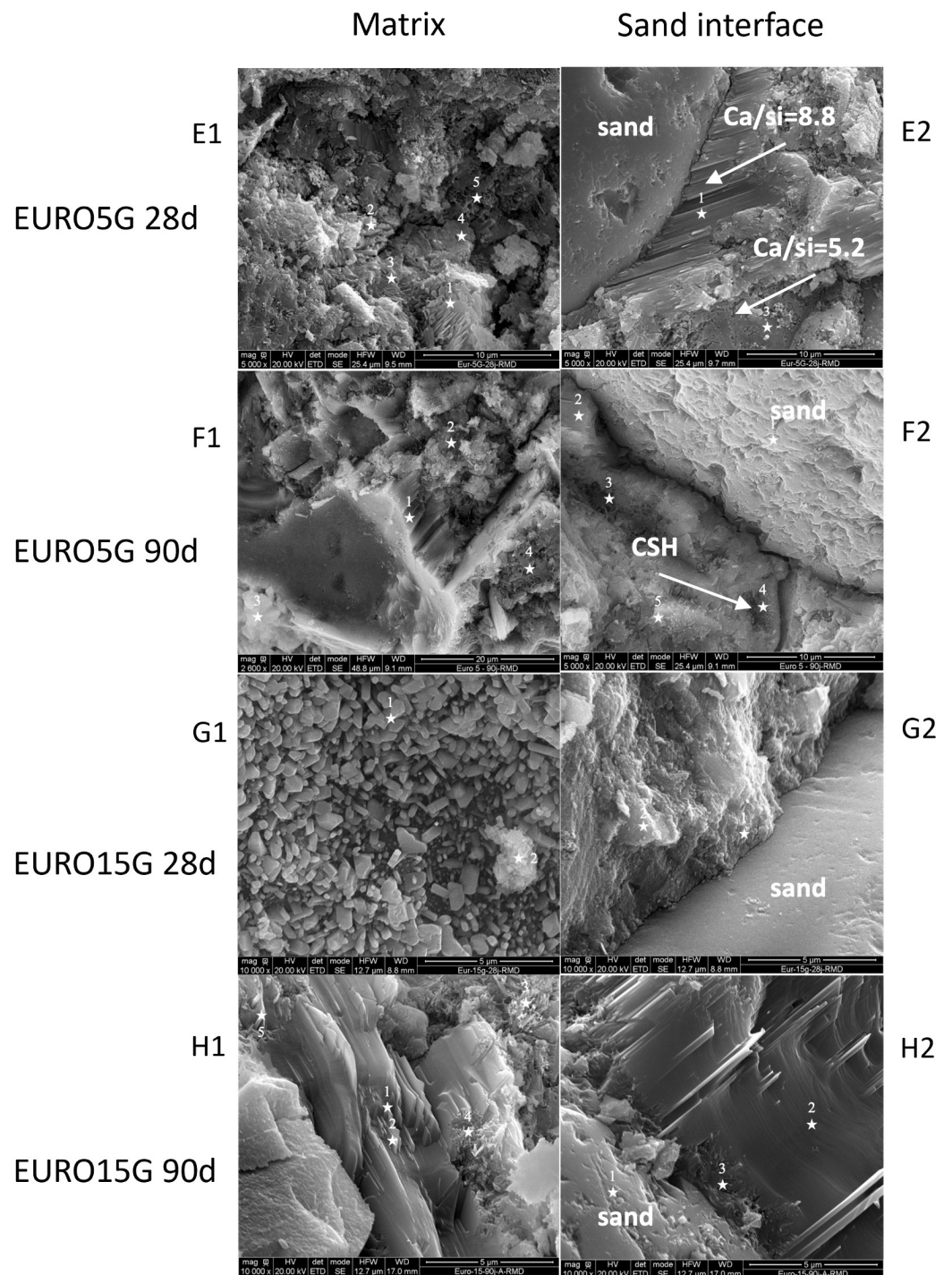


Figure 8. Cont.



**Figure 8.** SEM observations of 28- and 90-day mortars matrices and sand/matrix interface. Stars on the micrographs correspond to EDS targets and arrows point to characteristic mineral species ((C2) Magnification (M) = 1000; (A1,A2) M = 2500; (F1) M = 2600; (B1,B2,C1,D1,E1,E2,F2) M = 5000; (D2,G1,G2,H1,H2) M = 10,000).

The reference sample (A1 to B2) shows a densification of the matrix with the presence of microporosities at 28 days and their disappearance at 90 days. In images A1 and B1, there is a good distribution of Portlandite and CSH. In the vicinity of the sand grain, weakly polymerized CSH and Portlandite evolve at 90 days into an adhesive interface of CSH gel with Ca/Si between 1.2 and 2.2. The presence of mucilage in small quantities in the EURO2G images perfectly illustrates the impact of the polysaccharide on the cement

matrix. Image C1 shows a spherical geometric shape of CSH (Ca/Si of 2.6) surrounded by Portlandite that is particularly well ordered towards this sphere. This Portlandite organization is particularly visible and amplified on H1. This micrograph corresponds to a higher FM concentration, confirming the polysaccharides' influence on Portlandite structure. Knapen et al. [49] already observed this aligned arrangement of Portlandite because of polysaccharides. Image D1, despite the relatively long curing time, shows CSH and Portlandite forming, predominantly. The structure of the matrix remains particularly disordered and less dense than the reference. As far as the matrix around the sand grain is concerned, it consists mainly of Portlandite in the 28-day cure (C2), whereas in the 90-day cure, there is Portlandite and CSH at the same time (D2).

The increase in mucilage concentration (Figure 8) induces more and more morphological changes, confirming the arguments presented earlier. Image E1 shows that mucilage appears to influence CSH morphology since all the points analyzed in this image have Ca/Si values ranging from 2.2 to 2.9. At 90 days (F1), the evolution is notable, with Portlandite and CSH present. The matrix remains less dense than the reference matrix (B1) at the same age. The matrix/sand interface consists of Portlandite, as in mortar with less FM (C2). Indeed, image E2 shows Portlandite in two forms: one with a Ca/Si of 8.8 (close to the sand grain) and a Portlandite probably in the process of forming CSH, with a drop in Ca/Si = 5.2 (at distance of 6  $\mu\text{m}$  from the sand grain). Finally, EURO15G shows significant carbonation (G1) not seen in the other samples. The matrix is filled with  $\text{CaCO}_3$  at 28 days (G1), whereas in the 90-day cure, the matrix consists mainly of  $\text{Ca(OH)}_2$ , as the FM proportion is high. The observation of  $\text{Ca(OH)}_2$  in the matrix of the 90-day cure, when at 28 days  $\text{CaCO}_3$  was in the majority, has never been reported in the literature regarding low temperatures, but it is corroborated by Figure 7b showing that  $\text{CaCO}_3$  disappears in favor of  $\text{Ca(OH)}_2$ .

The shape of the Portlandite is particularly ordered (H1) and has a veiled appearance (H2). The veiled appearance is the result of the visualization of mucilage, as reported by Knapen et al. [49]. These authors clearly showed the interaction of polysaccharides with Portlandite in particular. Some organic additives have the ability to structure and make Portlandite durable. Usually, Portlandite is not able to resist the stresses of early cement hydration, but the very visible bonds between Portlandite and polysaccharides create a layer-like development of the Portlandite platelets. According to Knapen et al. [49], the presence of polymer bridges between the  $\text{Ca(OH)}_2$  crystals acts as an additional bond between the crystal layers and strengthens the crystal structure.

#### 3.2.4. Thermal Conductivities of Cement Mortars

The thermal conductivities (Figure 9) decrease as the mucilage amount increases. It is also obvious that thermal conductivities are largely related to the bulk density of mortars. This decrease in the bulk density is related to an increase in microstructural flocculation and internal porosity, as observed by SEM. Finally, the increase in the bulk density of EURO15G is related to the elaboration of the mortar. It is necessary to apply a different compaction on the fresh material in order to obtain a non-friable hardened mortar. This compaction leads to an increase in the bulk density and thermal conductivity of the material. This manual compaction during the elaboration of the EURO15G mortars is observed by a significant increase in the standard deviation of the bulk density of EURO15G, as the process is hardly reproducible.

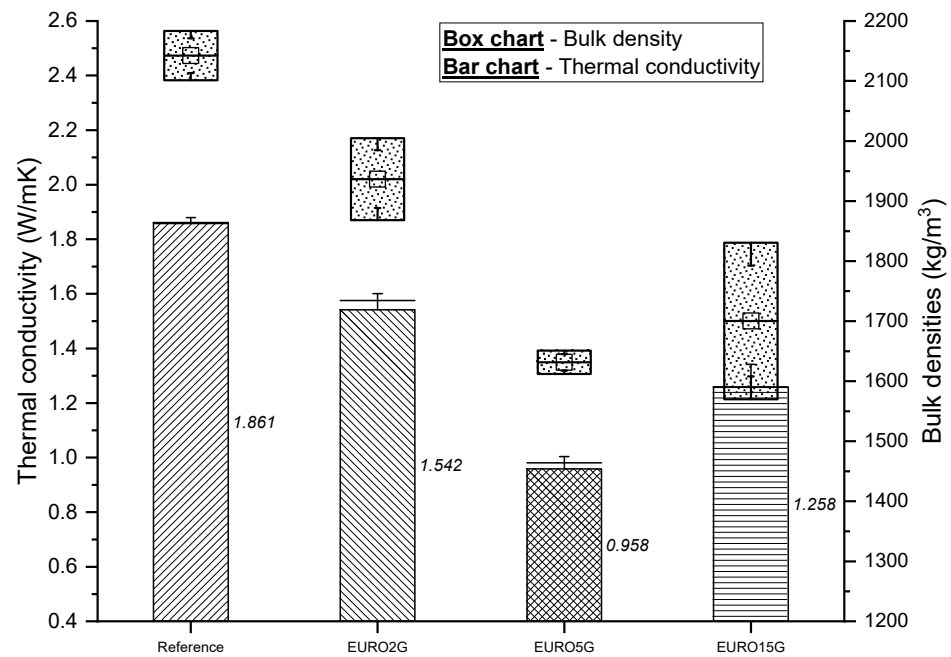


Figure 9. Thermal conductivities and bulk densities of 28-day cured mortars.

#### 4. Conclusions

The paper discusses the influence of the concentration of a co-product from a local waste: flaxseed mucilage. The study shows that the mucilage of flaxseed seems to show signs of degradation in a simulated cementitious environment, with a decrease in the apparent viscosity. This may be due to the elimination of hydrogen bonds governing the viscosity of the solution and a degradation of the conjugated products of the polysaccharide main chain.

The presented mucilage-admixed cement pastes study reveals that increasing the mucilage concentration delays drastically, even exponentially, the beginning and ending of cement setting. This delay is probably due to two main phenomena: (i) an increase in steric hindrance caused by a mucilaginous solution that is all the more viscous as it is concentrated and (ii) an increase, proportional to the amount of mucilage, in the absorption and chelation of cement  $\text{Ca}^{2+}$  ions by FM. The simultaneous effects lead to the decrease in the transport of the metal ions of the cement responsible for the nucleation of the CSH and the precipitation of the Portlandite. This delay lasts throughout the induction period. Later, a higher hydration acceleration is observed compared to the reference. The hydration degrees of the mortars are equivalent, whatever the formulation, proving the non-inhibition but delaying effect of the FM.

FM leads to cement flocculation, and the higher the FM concentration, the higher the flocculation. This flocculation induces an increase in porosity and a greater carbonation as well as a decrease in the compressive strength and thermal conductivity of the material. As demonstrated by other work from our group, this disorder can be eliminated by the use of a W/C ratio  $> 0.5$  at high admixture concentration (0.75% cement). Thus, not only the admixture rate but also the influence of the FM addition method (anhydrous and in-solution forms, a current work in progress) and the W/C ratio must be improved to better understand the potential of flaxseed mucilage in cementitious composites to target future applications.

As a highly hygroscopic material, FM can capture water and then release it gradually and under controlled conditions into the cement matrix over time. It would be interesting to verify that the regulation of water diffusion from the mucilage can induce self-healing properties. Effectively, by acting on cement grains not yet hydrated, this progressive release of water could produce new hydrates, thus reinforcing the mortar properties in the medium to long term. Another opportunity for valorizing mucilage would be to use a cement with a

lower Blaine fineness, which has a lower water requirement and slows down the evolution of the heat of hydration. A design of experiments combining admixture rate, W/C ratio, and cement type will enable more defined recommendations for the formulation of this type of mortar.

**Supplementary Materials:** The following supporting information can be downloaded at: <https://www.mdpi.com/article/10.3390/app14093862/s1>, Figure S1: SEC-MALS analysis of flaxseed mucilage ( $1 \text{ g}\cdot\text{L}^{-1}$ ) in NaOH solution (0.04 M) at different analysis times. (a) SEC-MALS profile (0 h: blue, 48 h: green and 72 h: red). Light curves are the molecular weight distribution, dark curves are the Refractive Index signal (RI). (b) SEC-MALS results (Mn: number average molecular weight, Mw: weight-average molecular weight, and polydispersity values (Mw/Mn)); Figure S2: SEC-MALS analysis of flaxseed mucilage ( $1 \text{ g}\cdot\text{L}^{-1}$ ) in  $\text{Ca}(\text{OH})_2$  solution (0.02 M) at different analysis times. (a) SEC-MALS profile (0 h: blue, 48 h: green and 72 h: red). Light curves are the molecular weight distribution, dark curves are the Refractive Index signal (RI). (b) SEC-MALS results (Mn: number average molecular weight, Mw: weight-average molecular weight, and polydispersity values (Mw/Mn).

**Author Contributions:** Conceptualization, H.B., E.P. and A.G.; methodology, H.B.; validation, E.P. and A.G.; formal analysis, H.B.; investigation, H.B., R.-M.D., N.M. and K.J.H.; resources, R.-M.D., N.M. and K.J.H.; data curation, H.B. and A.G.; writing—original draft preparation, H.B.; writing—review and editing, E.P. and A.G.; supervision, E.P. and A.G. All authors have read and agreed to the published version of the manuscript.

**Funding:** The French Ministry of Higher Education and Research supported this work through Haris Brevet's doctoral grant.

**Institutional Review Board Statement:** Not applicable.

**Informed Consent Statement:** Not applicable.

**Data Availability Statement:** Data will be made available on request.

**Acknowledgments:** The authors would like to acknowledge the support from Calcia for providing the Portland cement used in the study at a time when it was extremely difficult to obtain (post lockdown in France) and especially Bailly from Calcia Company. The authors also extend their appreciation and gratitude to Romain Roulard for the sugar composition analysis with HPAEC-PAD.

**Conflicts of Interest:** The authors declare that they have no known competing financial interests or personal relationships that could have appeared to influence the work reported in this paper.

## References

- Pirmohammadi, A.; Khalaji, S.; Yari, M. Effects of Linseed Expansion on Its Dietary Molecular Structures, and on Broiler Chicks Digestive Enzymes Activity, Serum Metabolites, and Ileal Morphology. *J. Appl. Poult. Res.* **2019**, *28*, 997–1012. [CrossRef]
- Chesneau, G.; Guillevic, M.; Germain, A.; Juin, H.; Lessire, M.; Enjalbert, F.; Burel, C.; Ferlay, A. Method for Treating Flax Seeds with a View to Improving the Value of Same. Patent WO 2019/101751 A1, 31 May 2019.
- Kaur, M.; Kaur, R.; Punia, S. Characterization of Mucilages Extracted from Different Flaxseed (*Linum usitatissimum* L.) Cultivars: A Heteropolysaccharide with Desirable Functional and Rheological Properties. *Int. J. Biol. Macromol.* **2018**, *117*, 919–927. [CrossRef]
- Fedeniuk, R.W.; Biliaderis, C.G. Composition and Physicochemical Properties of Linseed (*Linum usitatissimum* L.) Mucilage. *J. Agric. Food Chem.* **1994**, *42*, 240–247. [CrossRef]
- Shanmugavel, D.; Selvaraj, T.; Ramadoss, R.; Raneri, S. Interaction of a Viscous Biopolymer from Cactus Extract with Cement Paste to Produce Sustainable Concrete. *Constr. Build. Mater.* **2020**, *257*, 119585. [CrossRef]
- Thomas, N.L.; Birchall, J.D. The Retarding Action of Sugars on Cement Hydration. *Cem. Concr. Res.* **1983**, *13*, 830–842. [CrossRef]
- Hazarika, A.; Hazarika, I.; Gogoi, M.; Bora, S.S.; Borah, R.R.; Goutam, P.J.; Saikia, N. Use of a Plant Based Polymeric Material as a Low Cost Chemical Admixture in Cement Mortar and Concrete Preparations. *J. Build. Eng.* **2018**, *15*, 194–202. [CrossRef]
- Pan, J.; Feng, K.; Wang, P.; Chen, H.; Yang, W. Retardation and Compressive Strength Enhancement Effect of Upcycling Waste Carrot as Bio-Admixture for Cement Mortars. *J. Build. Eng.* **2022**, *62*, 105402. [CrossRef]
- Girones, J.; Vo, L.T.T.; Mouille, G.; Narciso, J.O.; Arnoult, S.; Brancourt-Hulmel, M.; Navard, P.; Lapiere, C. Impact of Miscanthus Lignin and Arabinoxylan on Portland Cement. *Ind. Crops Prod.* **2022**, *188*, 115585. [CrossRef]
- Hernández, E.F.; Cano-Barrita, P.D.J.; Torres-Acosta, A.A. Influence of Cactus Mucilage and Marine Brown Algae Extract on the Compressive Strength and Durability of Concrete. *Mater. Constr.* **2016**, *66*, e074. [CrossRef]
- Chandra, S.; Eklund, L.; Villarreal, R.R. Use of Cactus in Mortars and Concrete. *Cem. Concr. Res.* **1998**, *28*, 41–51. [CrossRef]

12. Azizi, C.E.; Hammi, H.; Chaouch, M.A.; Majdoub, H.; Mnif, A. Use of Tunisian *Opuntia ficus-indica* Cladodes as a Low Cost Renewable Admixture in Cement Mortar Preparations. *Chem. Afr.* **2019**, *2*, 135–142. [[CrossRef](#)]
13. Knapen, E.; Van Gemert, D. Cement Hydration and Microstructure Formation in the Presence of Water-Soluble Polymers. *Cem. Concr. Res.* **2009**, *39*, 6–13. [[CrossRef](#)]
14. Brevet, H.; Petit-Laignel, E.; Goullieux, A. Effects of Flaxseed Mucilage and Water to Cement Ratio on Mechanical and Hydration Characteristics of an OPC Mortar. *Acad. Mater. Sci.* **2023**, *1*, 1–10. [[CrossRef](#)]
15. Helrich, K. *Official Methods of Analysis of the AOAC*; AOAC: Rockville, MD, USA, 1990.
16. Roulard, R.; Petit, E.; Mesnard, F.; Rhazi, L. Molecular Investigations of Flaxseed Mucilage Polysaccharides. *Int. J. Biol. Macromol.* **2016**, *86*, 840–847. [[CrossRef](#)] [[PubMed](#)]
17. AFNOR NF EN 196-1; Methods of Testing Cement. Part 1: Determination of Strength. Normes et Normalisation Européenne: Brussels, Belgium, 2016.
18. Schwartzentruber, A.; Catherine, C. La Méthode Du Mortier de Béton Équivalent (MBE)—Un Nouvel Outil d'aide à La Formulation Des Bétons Adjuvantés. *Mater. Struct.* **2000**, *33*, 475. [[CrossRef](#)]
19. Bhatti, J.I. Hydration versus Strength in a Portland Cement Developed from Domestic Mineral Wastes—A Comparative Study. *Thermochim. Acta* **1986**, *106*, 93–103. [[CrossRef](#)]
20. Zhang, Q.; Ye, G. Dehydration Kinetics of Portland Cement Paste at High Temperature. *J. Therm. Anal. Calorim.* **2012**, *110*, 153–158. [[CrossRef](#)]
21. El-Jazairi, B.; Illston, J. The Hydration of Cement Paste Using the Semi-Isothermal Method of Derivative Thermogravimetry. *Cem. Concr. Res.* **1980**, *10*, 361–366. [[CrossRef](#)]
22. Hellebois, T.; Fortuin, J.; Xu, X.; Shaplov, A.S.; Gaiani, C.; Soukoulis, C. Structure Conformation, Physicochemical and Rheological Properties of Flaxseed Gums Extracted under Alkaline and Acidic Conditions. *Int. J. Biol. Macromol.* **2021**, *192*, 1217–1230. [[CrossRef](#)]
23. Hadad, S.; Goli, S.A.H. Fabrication and Characterization of Electrospun Nanofibers Using Flaxseed (*Linum usitatissimum*) Mucilage. *Int. J. Biol. Macromol.* **2018**, *114*, 408–414. [[CrossRef](#)]
24. de Paiva, P.H.E.N.; Correa, L.G.; Paulo, A.F.S.; Balan, G.C.; Ida, E.I.; Shirai, M.A. Film Production with Flaxseed Mucilage and Polyvinyl Alcohol Mixtures and Evaluation of Their Properties. *J. Food Sci. Technol.* **2021**, *58*, 3030–3038. [[CrossRef](#)] [[PubMed](#)]
25. Warrand, J. Etude Structurale et Propriétés en Solution des Polysaccharides Constitutifs du Mucilage de lin (*Linum usitatissimum* L.). Ph.D. Thesis, University of Picardie Jules Verne, Amiens, France, 2004.
26. Emaga, T.H.; Rabetafika, N.; Blecker, C.S.; Paquot, M. Kinetics of the Hydrolysis of Polysaccharide Galacturonic Acid and Neutral Sugars Chains from Flaxseed Mucilage. *Biotechnol. Agron. Soc. Environ.* **2021**, *16*, 139–147.
27. Lefsih, K.; Delattre, C.; Pierre, G.; Michaud, P.; Aminabhavi, T.M.; Dahmoune, F.; Madani, K. Extraction, Characterization and Gelling Behavior Enhancement of Pectins from the Cladodes of *Opuntia ficus indica*. *Int. J. Biol. Macromol.* **2016**, *82*, 645–652. [[CrossRef](#)] [[PubMed](#)]
28. Yu, L.; Stokes, J.R.; Yakubov, G.E. Viscoelastic Behaviour of Rapid and Slow Self-Healing Hydrogels Formed by Densely Branched Arabinoxylans from *Plantago Ovata* Seed Mucilage. *Carbohydr. Polym.* **2021**, *269*, 118318. [[CrossRef](#)] [[PubMed](#)]
29. Zhou, P.; Eid, M.; Xiong, W.; Ren, C.; Ai, T.; Deng, Z.; Li, J.; Li, B. Comparative Study between Cold and Hot Water Extracted Polysaccharides from *Plantago Ovata* Seed Husk by Using Rheological Methods. *Food Hydrocoll.* **2020**, *101*, 105465. [[CrossRef](#)]
30. Chen, H.-H.; Xu, S.-Y.; Wang, Z. Gelation Properties of Flaxseed Gum. *J. Food Eng.* **2006**, *77*, 295–303. [[CrossRef](#)]
31. Pourchez, J.; Govin, A.; Grosseau, P.; Guyonnet, R.; Guilhot, B.; Ruot, B. Alkaline Stability of Cellulose Ethers and Impact of Their Degradation Products on Cement Hydration. *Cem. Concr. Res.* **2006**, *36*, 1252–1256. [[CrossRef](#)]
32. Jayasingh, S.; Selvaraj, T. Influence of Organic Additive on Carbonation of Air Lime Mortar—Changes in Mechanical and Mineralogical Characteristics. *Eur. J. Environ. Civ. Eng.* **2022**, *26*, 1776–1791. [[CrossRef](#)]
33. Ponder, G.; Richards, G. Arabinogalactan from Western Larch, Part III: Alkaline Degradation Revisited, with Novel Conclusions on Molecular Structure. *Carbohydr. Polym.* **1997**, *34*, 251–261. [[CrossRef](#)]
34. Jing, Y.; Zhu, J.; Liu, T.; Bi, S.; Hu, X.; Chen, Z.; Song, L.; Lv, W.; Yu, R. Structural Characterization and Biological Activities of a Novel Polysaccharide from Cultured *Cordyceps Militaris* and Its Sulfated Derivative. *J. Agric. Food Chem.* **2015**, *63*, 3464–3471. [[CrossRef](#)]
35. Biermann, C.J. Hydrolysis and Other Cleavages of Glycosidic Linkages in Polysaccharides. *Adv. Carbohydr. Chem. Biochem.* **1988**, *46*, 251–271. [[CrossRef](#)]
36. Kang, X.; Wang, Y.-Y.; Wang, S.; Song, X. Xylan and Xylose Decomposition during Hot Water Pre-Extraction: A pH-Regulated Hydrolysis. *Carbohydr. Polym.* **2021**, *255*, 117391. [[CrossRef](#)] [[PubMed](#)]
37. Whistler, R.L.; BeMiller, J. Alkaline Degradation of Polysaccharides. In *Advances in Carbohydrate Chemistry*; Elsevier: Amsterdam, The Netherlands, 1958; Volume 13, pp. 289–329.
38. León-Martínez, F.; Cano-Barrita, P.D.J.; Lagunez-Rivera, L.; Medina-Torres, L. Study of Nopal Mucilage and Marine Brown Algae Extract as Viscosity-Enhancing Admixtures for Cement Based Materials. *Constr. Build. Mater.* **2014**, *53*, 190–202. [[CrossRef](#)]
39. Dickinson, E.; Eriksson, L. Particle Flocculation by Adsorbing Polymers. *Adv. Colloid Interface Sci.* **1991**, *34*, 1–29. [[CrossRef](#)]
40. Zhang, L.; Catalan, L.J.; Balec, R.J.; Larsen, A.C.; Esmaeili, H.H.; Kinrade, S.D. Effects of Saccharide Set Retarders on the Hydration of Ordinary Portland Cement and Pure Tricalcium Silicate. *J. Am. Ceram. Soc.* **2010**, *93*, 279–287. [[CrossRef](#)]
41. Bruere, G.M. Set-Retarding Effects of Sugars in Portland Cement Pastes. *Nature* **1966**, *212*, 502–503. [[CrossRef](#)]

42. Young, J. A Review of the Mechanisms of Set-Retardation in Portland Cement Pastes Containing Organic Admixtures. *Cem. Concr. Res.* **1972**, *2*, 415–433. [[CrossRef](#)]
43. Martínez-Molina, W.; Torres-Acosta, A.; Martínez-Peña, G.I.; Guzmán, E.A.; Mendoza-Pérez, I. Cement-Based, Materials-Enhanced Durability from *Opuntia ficus indica* Mucilage Additions. *ACI Mater. J.* **2015**, *112*, 165. [[CrossRef](#)]
44. Torres-Acosta, A.A.; González-Calderón, P.Y. *Opuntia ficus-indica* (OFI) Mucilage as Corrosion Inhibitor of Steel in CO<sub>2</sub>-Contaminated Mortar. *Materials* **2021**, *14*, 1316. [[CrossRef](#)]
45. León-Martínez, F.; Cano-Barrita, P.D.J.; Castellanos, F.; Luna-Vicente, K.; Ramírez-Arellanes, S.; Gómez-Yáñez, C. Carbonation of High-Calcium Lime Mortars Containing Cactus Mucilage as Additive: A Spectroscopic Approach. *J. Mater. Sci.* **2021**, *56*, 3778–3789. [[CrossRef](#)]
46. Wang, J.; Xu, H.; Xu, D.; Du, P.; Zhou, Z.; Yuan, L.; Cheng, X. Accelerated Carbonation of Hardened Cement Pastes: Influence of Porosity. *Constr. Build. Mater.* **2019**, *225*, 159–169. [[CrossRef](#)]
47. Janotka, I.; Madejová, J.; Števula, L.; Fri'álová, D.M. Behaviour of Ca(OH)<sub>2</sub> in the Presence of the Set Styrene-Acrylate Dispersion. *Cem. Concr. Res.* **1996**, *26*, 1727–1735. [[CrossRef](#)]
48. Silva, D.A.; Roman, H.R.; Gleize, P.J.P. Evidences of Chemical Interaction between EVA and Hydrating Portland Cement. *Cem. Concr. Res.* **2002**, *32*, 1383–1390. [[CrossRef](#)]
49. Knapen, E.; Van Gemert, D. Polymer Film Formation in Cement Mortars Modified with Water-Soluble Polymers. *Cem. Concr. Compos.* **2015**, *58*, 23–28. [[CrossRef](#)]

**Disclaimer/Publisher's Note:** The statements, opinions and data contained in all publications are solely those of the individual author(s) and contributor(s) and not of MDPI and/or the editor(s). MDPI and/or the editor(s) disclaim responsibility for any injury to people or property resulting from any ideas, methods, instructions or products referred to in the content.